

Recent Application of Weather Radar Observation into Hydrologic Forecasting in Japan

Eiichi Nakakita and Sunmin Kim

Abstract This paper introduces recent research efforts on hydrologic flood forecasting in Japan using multiple weather radar observation networks. After illustrating the details of weather radar observation systems in Japan, several noticeable researches of the authors are introduced.

Keywords Weather radar · X-band · C-band · Dual polarization · Early detection · Rain cell · Flood forecasting · Ensemble forecasting

1 Introduction

Advances in weather radar observation techniques have allowed us to expect significant improvement in flash flood forecasting with a distributed hydrologic model. More accurate and localized flood predictions (in terms of estimating flood peak time and magnitude) are now available, by applying state-of-the-art knowledge and technology to hydrology and meteorology. Weather radar has been a widely used tool for precipitation observation for the last several decades, and much research effort has been applied to improve the accuracy of quantitative precipitation estimation (QPE) and quantitative precipitation forecasting (QPF) using weather radar (e.g., [1, 3, 7]).

The radar observation system in Japan is operated by two governmental groups: Japan Meteorological Agency (JMA) and the Ministry of Land, Infrastructure, Transport and Tourism (MLIT) of Japan. The JMA radar observation network is

E. Nakakita (✉)
Disaster Prevention Research Institute, Kyoto University, Gokasyo,
Uji, Kyoto, Japan
e-mail: nakakita@hmd.dpri.kyoto-u.ac.jp

S. Kim
Graduate School of Engineering, Kyoto University, KyotoDaigakuKatsura,
Kyoto, Japan
e-mail: kim.sunmin.6x@kyoto-u.ac.jp

comprised of 20 C-band radars (with a wavelength of 5.6 cm), which cover most of the Japan Islands and observe rainfall intensity and distribution. Radar data are digitized to produce special radar echo composite maps every five minutes for the purpose of monitoring precipitation throughout the country. The data are also calibrated using the gauged point rainfall intensities. On the other hand, the MLIT's radar observation system is composed of 26 C-band radars throughout Japan. The observed radar echo from each radar unit is first modified and then sent to the National Bureau of Synthesis Process within the MLIT. Through several steps for homogenizing observation accuracy, including distance and elevation correction, synthesized rainfall intensity maps for the entire nation of Japan are generated every five minutes.

Those two radar networks of Japan are characterized by their respective observation purposes. The radar observation conducted by the JMA is intended to provide basic information for short-term precipitation forecasting. Thus, it focuses on rainfall distribution and is therefore more sensitive in order to capture the low rainfall intensity values. On the other hand, the observation conducted by the MLIT is intended to assist the flood forecasting system of the River Bureau, MLIT, and is focused on capturing an accurate measurement of rainfall intensities during heavy rainfall. As will be discussed in the following section, the conventional C-band radar observation conducted by the MLIT tends to overestimate rainfall intensities.

The MLIT has recently launched a new radar observation network system designed for flash flood observation and forecasting in small river basins within urban areas. It is called the X-band multi-parameter radar network and is distinguished by its dual polarimetric wave pulses of short length (3 cm). Attenuation problems resulting from the short wave length of radar echo are strengthened by polarimetric wavelengths and very dense radar networks. In total, 39 X-band MP radars have been established around many cities in Japan by 2015, since it was first introduced in 2009. Each observation in area around many cities is conducted by 3–4 X-band radars with very fine spatial resolution (250 m) in every one minute.

The details of the X-band radar network are summarized in Table 1, comparing it with the conventional C-band radar observation conducted by the JMA and the

Table 1 Characteristics of each radar observation in Japan

Details	C-band radar network of the JMA	C-band radar network of the MLIT	X-band radar network of the MLIT
Observation interval (min)	10	5	1
Data distribution (min)	5–10	5–10	1–2
Spatial resolution	1 km	1 km	250 m
Wave length (cm)	5–6	5–6	3
Observation range	120 km radius	120 km radius	60 km radius
Dual polarization	No	Partially	Yes
Doppler function	Partially	Partially	Yes
Volume scanning	Yes	Partially	Yes

MLIT. While conventional radar observation takes 10–15 min to observe, collect, and distribute the information to the public, the new radar networks require only 2–3 min for full distribution. At the present time, the observation network is in a testing phase for operational usage, checking the observation accuracy and applicability in a wide variety of aspects.

2 Utilization of X-Band MP Radar

2.1 Background of XRAIN Utilization

On July 28, 2008, about 50 people who were enjoying a sunny day along a small river channel (Toga-gawa) near their residential area in Kobe City, Japan, were swept away by a flash flood caused by the sudden development of a convective rainstorm; five were later found dead. It took only 16 min for the water level of the channel to increase 1.4 meters after the rainstorm started in the small, 8.7 km² catchment area [6].

Later, it was found that a single cumulonimbus cloud developed about 30 min before the heavy rain started and induced the flash flood [2]. In the same year, another five people working in an underground sewage pipe system in Tokyo City were swept away and lost their lives because of flash flood in an urbanized area induced by a suddenly developed cumulonimbus cloud.

Intensive investigations and research were done to figure out the exact procedure of the tragic accidents and to prevent those kinds of disasters in the future. Among the information, the first echo of the Toga-gawa rainstorm event was detected with a three-dimensional volume scan image from a C-band radar [2]. The first echo of the rainstorm was detected at a 5 km height in the atmosphere at 14:14 p.m. that day, which was 15 min before the rain started on the ground and 31 min before the flash flood occurred.

Even considering a certain amount of time lapsed for a warning to be issued and evacuation to occur, this early detection could have provided enough time to save all those people. There have been continuous research efforts to provide precise short-term rainfall forecasting based on real-time radar observation data (e.g., [1, 3]) as well as combining with numerical weather prediction model outputs (e.g., [7]). However, the conventional nowcasting skills are not able to predict such a suddenly developed convective rainstorm, since the conventional methods are based on already developed rainstorms.

Meanwhile, as a nationwide countermeasure, the Japanese government has been installing a new weather radar network called X-band polarimetric radar information network (XRAIN) around the major urban areas in Japan since 2010 to prevent flash flood disasters with more accurate and faster observations of rainstorms. For the last 4 years, the Ministry of Land, Infrastructure, Transport and Tourism (MLIT) of Japan has equipped 14 major cities, including Tokyo, Nagoya, Osaka, and Kobe, with 39 XRAIN radars (see Fig. 1).

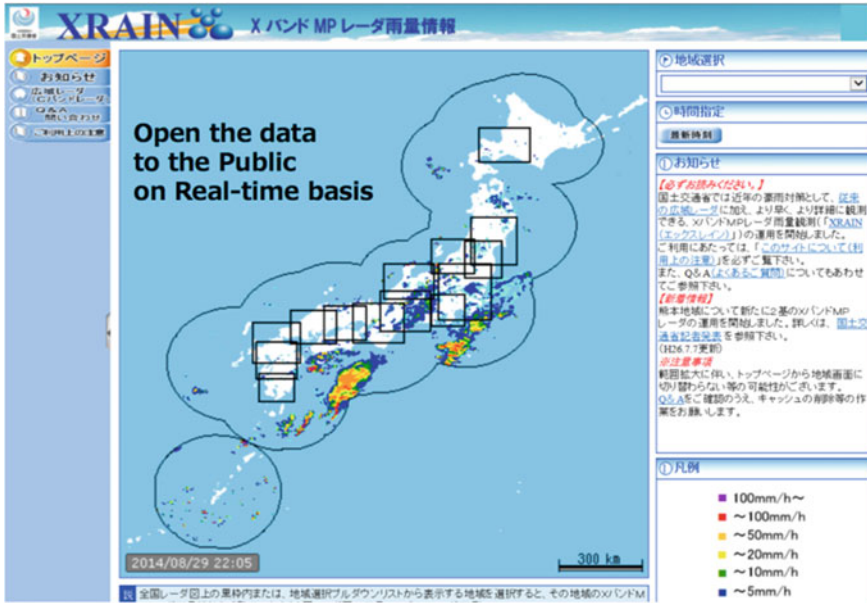


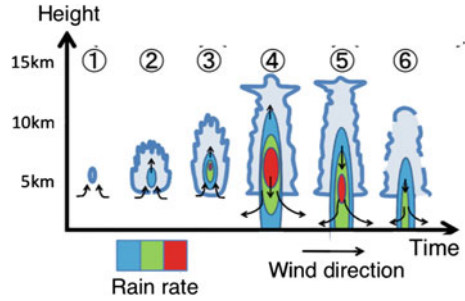
Fig. 1 Screen shot of XRAIN Web site to public. Solid rectangular line shows 14 areas covered by 39 XRAIN radars

The XRAIN radar is characterized by high spatial resolution (250 m) and frequent observation interval (1-minute) with X-band wavelengths (3 cm) within the densely overlapped observation network, allowing us to overcome the attenuation and short observation range problems. The dual-polarized radio waves of XRAIN provide improved polarimetric functions, such as ZDR and KDP, which provide higher accuracy of quantitative precipitation estimations (QPEs) compared to the conventional QPE based on the Z–R relationship. Superiority of polarimetric weather radar has been well known for its improved accuracy of QPEs as well as its applicability for detecting hazardous convective rainstorms. Additionally, Doppler velocity of rain cells is observed with three-dimensional volume scanning. One of the best merits of XRAIN is that it takes only one minute to get the composed horizontal distribution of rainfall intensity from the observation network, and one cycle of the three-dimensional volume scan is available every five minutes.

2.2 Early Detection of Baby Rain cell

Based on the newly equipped radar observation network of Japan, our research team has been developing an effective algorithm to detect a baby rain cell, which is the early stage of a single-cell rainstorm (refer to Fig. 2). The definition of a

Fig. 2 Radar depiction of a rainstorm, showing life cycle of radar cross section. Early detection algorithm is able to detect the first echo in the stage of 1 or 2 and is also able to evaluate whether it will be developed to heavy rainfall



single-cell rainstorm in this study is a rainstorm generated from an independently developed cumulonimbus cloud having more than 50 mm/h of rainfall intensity. The criteria to select baby rain cells from numerous radar echoes are set empirically as a first echo having more than 20 dBZ of intensity when there was no precedent reflectivity in the previous volume scan (5 min before) within a 5 km radius. The reflectivity criteria were set as a relatively low value to detect very early stages of baby rain cells while trying to avoid interruption from noise echo.

The microscale vortex in the early stage of rainstorms was observed in our previous study [4], and it was able to estimate pseudo-vorticity using the Doppler velocity observation. Based on the introduced early detection algorithm, it was able to detect baby rain cells 5–15 min before their development, and it was successful at determining the danger level for whether the rain cells would finally downpour to the ground as heavy rainfall (see Fig. 3).

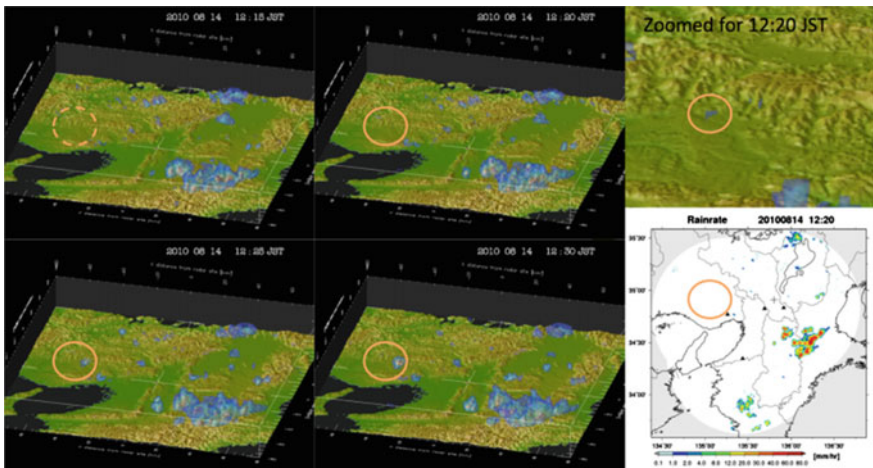


Fig. 3 An example of a detected baby rain cell at 12:20 p.m. on Aug. 14, 2010. The baby rain cell was first detected at 12:20 p.m. (*upper right*), while there was no rainfall on the ground yet (*bottom right*). The baby rain cell showed its increased volume and reflectivity strength while it moved eastward between 12:25 p.m. and 12:30 p.m. (*bottom left and bottom center*)

The evaluation results from the collected 35 single-cell rainstorm events so far showed that every event had a strong vertical vorticity in the early stage of its evolution. Average time until the first detection of vorticity was 1.7 min after the detection of baby rain cells, while the average time of maximum rainfall intensity appeared 25.3 min after the detection of baby rain cells. In the end, vorticity detection occurred 23.6 min before the maximum rainfall intensity on the ground.

Currently, an automatic rainstorm nowcasting system is under developing based on the baby rain cell detection and the vorticity estimation algorithm. The purpose of the rainstorm nowcasting system development is to provide early warnings of single-cell rainstorms even before it starts to rain. The major algorithm of the system is divided into three steps: (1) to detect a baby rain cell in the early stage of a single-cell rainstorm, (2) to decide its danger level with the vorticity estimation, and (3) to trace the baby rain cell until it develops into a rainstorm and finally disappears.

It is noteworthy that only 10 min or even 5 min of earlier detection could give us enough time to save lives from a natural disaster. And, the presented algorithm and system are based on the ongoing collaborative research with the Ministry of Land, Infrastructure, Transport and Tourism (MLIT) of Japan, with continuous upgrading of the equipped XRAIN observation system.

3 Ensemble Forecasting with Multiple Input

3.1 Combination of X-Band and C-Band Radar Input

This study is designed to evaluate the new radar observation network from a hydrologic perspective. First of all, the accuracy of the X-band radar observation was determined by comparing its results with the rainfall intensities as observed by ground gauge stations. It was also compared with conventional C-band radar observation of MLIT. The rainfall information from the new radar network was then provided to a distributed hydrologic model to simulate river discharges. The simulated river discharges were evaluated again using the observed river discharge to estimate the applicability of the new observation network in the context of operations regarding flood forecasting.

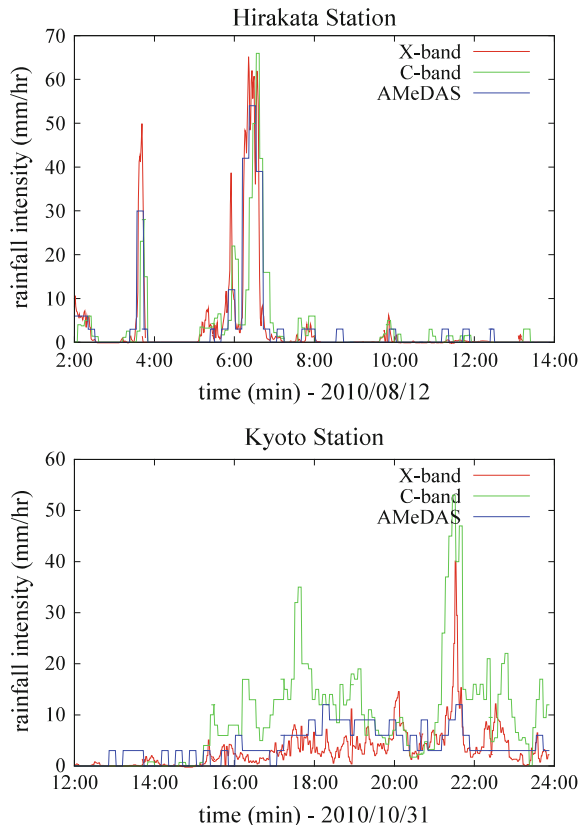
The tested rainfall data in this study, which was derived from X-band radar and the conventional C-band radar, are provided by the MLIT as synthesized rainfall intensities within rectangular coordinates. However, both data sets are not bias corrected using the ground-gauged data. We adopted an already-built-up rainfall–runoff simulation system on the Yodo River Basin of Japan for the hydrologic evaluation of the radar-observed rainfall data. The Yodo River Basin is in the Kansai District, located in the midwest region of Japan, and is one of the X-band observation networks covering the river basin (the sixth rectangular section from the left in Fig. 1). Details of the selected events are provided in Table 2.

Table 2 Rainfall event utilized in hydrologic evaluation

Event	Event duration	Maximum rainfall intensity
Event 1	02:00–14:00, Aug. 12, 2010	Up to 50 mm/h
Event 2	00:00–18:00, Oct. 09, 2010	20–30 mm/h
Event 3	12:00–24:00, Oct. 31, 2010	10–20 mm/h

Ground gauging observation data from the AMeDAS were collected for the evaluation of the X-band radar observation’s accuracy. Ten gauging stations are available within the X-band observation network of the Kansai District. Each AMeDAS observation station offers 10-min intervals of rainfall intensity data, and this data were utilized to evaluate both the X-band radar observation and the C-band radar observation. Figure 4 shows an example of the comparison of the rainfall intensities observed by the AMeDAS ground gauging station, X-band, and C-band radar networks. As the representative example shown in Fig. 4 (up), both observations made by the X-band radar and the C-band radar show a high degree of agreement and accuracy when compared to the ground gauge station values. However, the C-band radar observations show overestimated values in many cases,

Fig. 4 Rainfall intensity comparison using the X-band radar and C-band radar observations compared to the observations at the ground gauging stations (AMeDAS) of Hirakata (up) and Kyoto (down)



and the X-band radar observations provide underestimated rainfall intensities in some cases.

The rainfall information gathered from the both radar observations was evaluated from a hydrologic perspective. Both rainfall input data sets were provided to the hydrologic model and the simulated river discharges were compared with the observed discharge data to determine the input accuracy. The hydrologic model utilized here was a physically based distributed hydrologic model using one-dimensional kinematic wave equation. For the hillslope runoff simulation using 250-m resolution DEM, the model utilizes the kinematic wave equation, which incorporates a stage discharge relationship for subsurface and surface flow. Channel flow simulation was also conducted by solving the kinematic wave equation and the model produced hourly based hydrographs at each river segment.

The hydrologic model was calibrated manually using the observed point-gauged rainfall data and river discharge data from the Yodo River Basin. There are five parameters to be optimized in the model: roughness coefficient n , soil depths d_s and d_c , and hydraulic conductivities k_a and k_c [5]. For the evaluation of the radar-observed rainfall data, inflows at the multiple dam sites were simulated using the distributed hydrologic model. Figure 5 (up) shows one of the typical simulation results and their comparison with the observed river discharge at both checkpoints.

The X-band radar-observed rainfall data provide very good simulation results in most cases when those are compared to the observed discharges. The simulation results using the C-band radar-observed rainfall data also give considerably good simulation results. However, the accuracy of the simulation results is diverse in each event and each catchment.

According to the evaluation test on the both radar observations, it was able to understand that the newly equipped X-band polarimetric radar network shows somewhat improved observation accuracy compared to conventional C-band radar observation. However, it has a tendency to underestimate the rainfall, and the accuracy is not always superior to that of the C-band radar.

Based on the evaluation information, we have tested couple of methods to blend the advantages of the both radar networks, one is to synthesize the radar-observed rainfall intensities and the other one is to synthesize the simulated river discharges from each rainfall information. It was found that the both blending methods show improved forecasting accuracy compared to the independent utilization of radar information as shown in Fig. 5 (down).

3.2 Combination of Radar Observation and NWP Output

Many river basins in Japan are characterized by steep mountains in many regions, which are generating orographic rainfall significantly. Because of this orographic effect in the rainfall, it was not easy to get good enough accuracy of radar-based rainfall prediction. To overcome this prediction huddle, [3] proposed an improved radar image extrapolation method by combining orographic rainfall identification

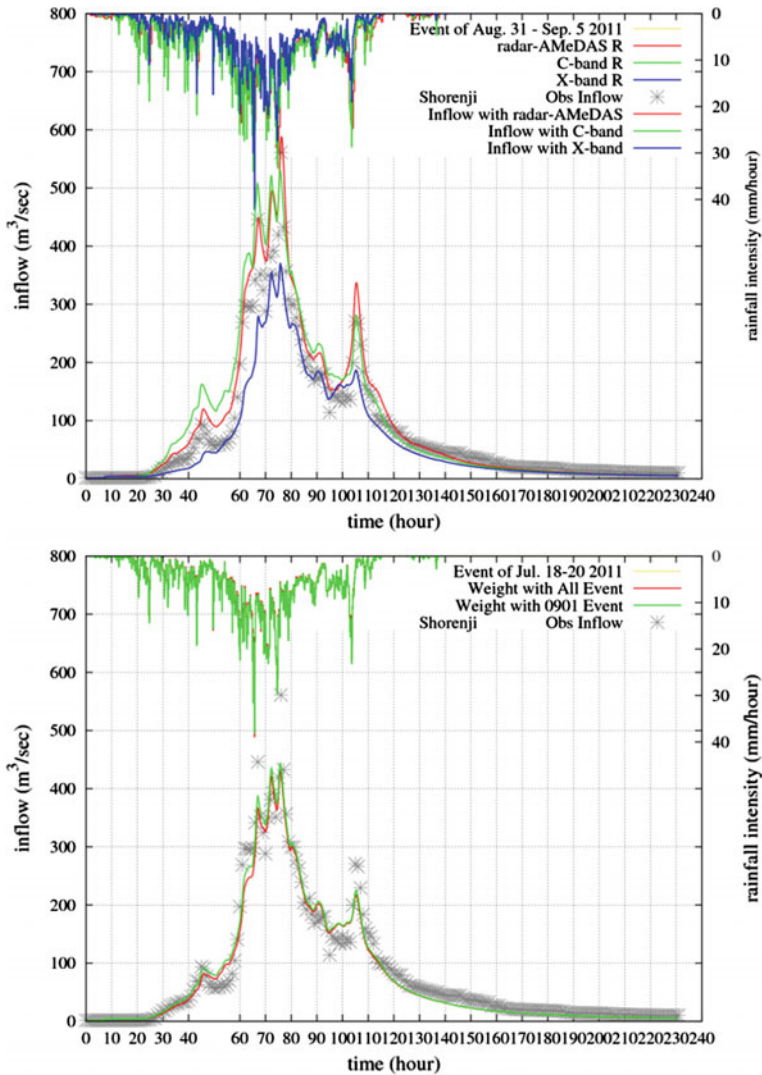


Fig. 5 Runoff simulation results with independent utilization of radar information (*left*) and with the blended radar information (*right*) that shows improved forecasting accuracy

scheme and the error-field scheme considering prediction error structures (Fig. 6). The method was able to improve the prediction accuracy in mountainous areas by separating radar rainfall into orographic and non-orographic rain fields. And consideration of future prediction error using the characteristics of the recent prediction error has been showing robust accuracy improvements [1, 3].

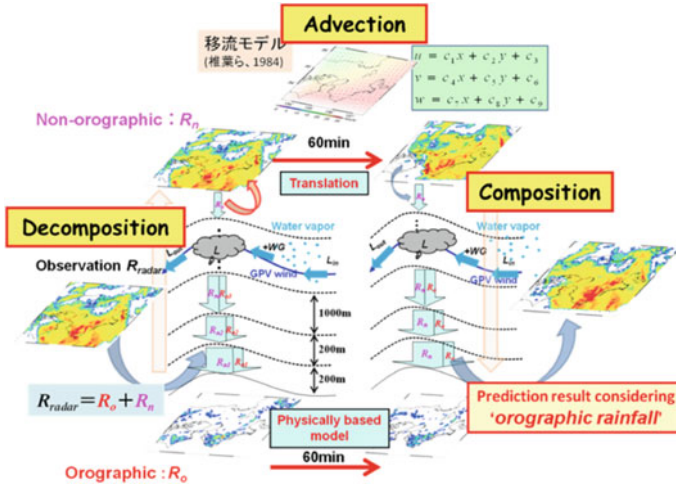


Fig. 6 Schematic drawing of delineation for orographic rainfall amounts [3]

However, the accuracy of radar-based rainfall prediction decreases drastically while the prediction lead time getting longer. It is generally believed that the radar image extrapolation method is proper for short lead time, e.g., up to 3 h. As an alternative to provide longer lead time predictions, QPFs from NWP models are widely utilized. NWP (numerical weather prediction) models simulate the dynamics and physics of the atmosphere, and therefore, they are able to produce more reliable forecasts over longer lead times.

The combination of radar-based prediction with NWP model output, which is known as hybrid forecasting scheme, has been provided for the last several decades. The combination of the data is based on the merging of rainfall prediction outputs through radar image extrapolation method with outputs of an NWP model. Hybrid forecasting of radar-based prediction with NWP rainfall has shown that it provides more skillful forecasts than either NWP forecast or radar prediction alone. However, the accuracy improvement of each prediction method with NWP and radar prior to blending technique has not been addressed well in the related previous researches.

The main objective of this study was to blend the advantages of ensemble information of radar-based prediction with NWP rainfall for the accuracy improvement of rainfall and flood forecasting using the hybrid forecasting scheme. At first, the accuracy of radar image extrapolation method is improved by considering orographic rainfall identification and the error-field updating scheme. The accuracy of ensemble NWP output was also improved by utilizing the error-field updating scheme based on the concept of [1] (Fig. 7).

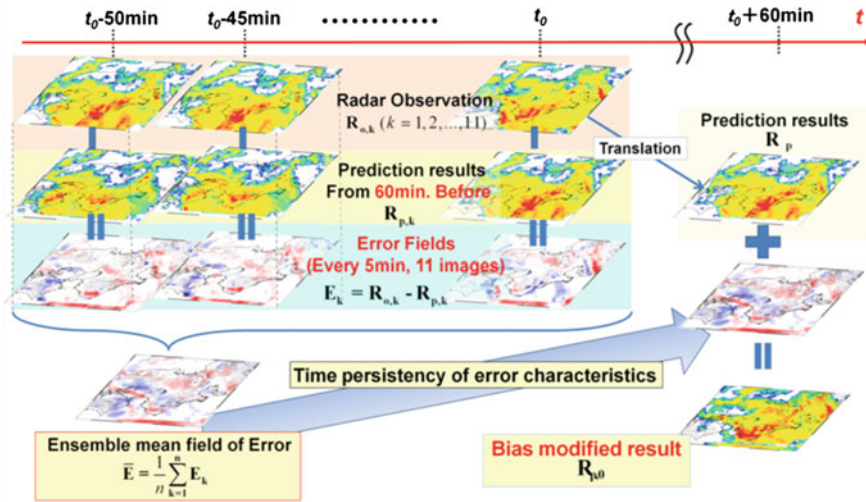


Fig. 7 Schematic drawing for the error-field update scheme in the radar image extrapolation method [1]

Finally, improved radar-based prediction and updated ensemble NWP rainfall forecast were merged with a time-variant weight function through Critical Success Index (CSI) and root mean square error (RMSE) indexes from the previous 3 h forecasting results. The proposed blending method was verified through 2011’s largest rainfall event for Typhoon Talas and was applied to the hybrid flood forecasting on dam catchments in Kii Peninsula, Japan.

Based on the successful application results, improved radar image extrapolation method with the consideration of orographic rainfall identification and the error fields showed better performance than other radar prediction methods in spatial forecast location in verification results of accumulated rainfall distribution, correlation coefficient, CSI, and RMSE indexes. And ensemble NWP rainfall was improved with quantitative bias correction using mean field bias of error fields, and updated NWP rainfall produced higher performances than radar prediction results considering the orographic rainfall and the error-field scheme.

The improvement achieved by merging the radar prediction with the updated NWP rainfall becomes prominent for longer lead times and for stronger rainfall intensities in case of both the error-field schemes. And hybrid flood forecasting with combination of blending and updated NWP rainfall by error-field scheme could improve the underestimated part of original ensemble NWP rainfall in rising limb and peak discharge period over the two catchments (Fig. 8). In overall, the bias correction by error-field scheme added to each ensemble member appears to significantly enhance the ensemble’s utility and provide a more effective way for accuracy improvement in rainfall and flood forecasting in the subject basin.

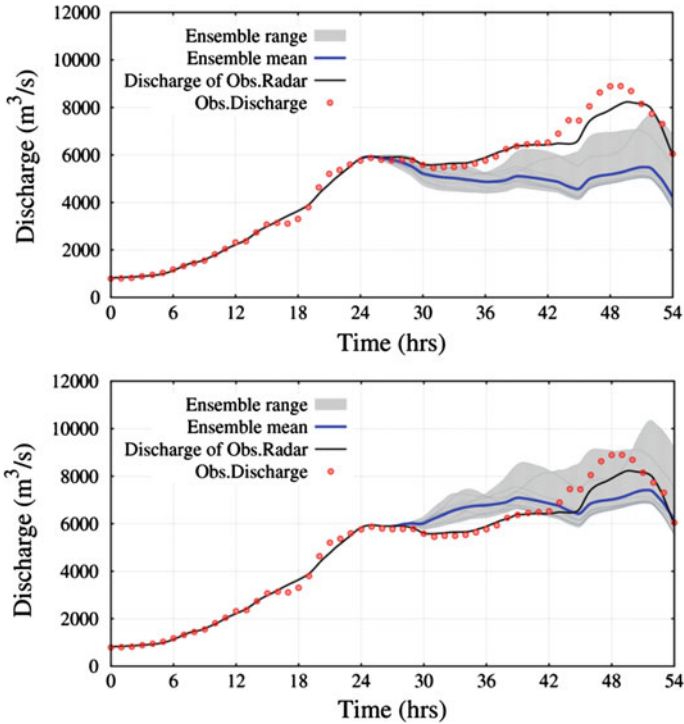


Fig. 8 Runoff simulation results with NWP ensemble output without error correction and blending scheme (*up*) and with the blended radar information (*down*) that shows improved forecasting accuracy

References

1. Kim S, Tachikawa Y, Sayama T, Takara K (2009) Ensemble flood forecasting with stochastic radar image extrapolation and a distributed hydrologic model. *Hydrol Process* 23:597–611. doi:[10.1002/hyp.7188](https://doi.org/10.1002/hyp.7188)
2. Nakakita E, Yamabe H, Yamaguchi K (2010) Earlier detection of the origin of very localized torrential rainfall. *J Hydraul Eng JSCE* 54:343–348
3. Nakakita E, Yoshikai T, Kim S (2012) Application of error-ensemble prediction method to a short-term rainfall prediction model considering orographic rainfall. *Weather Radar Hydrol* 351:317–322
4. Nakakita E, Nishiwaki R, Yamabe H, Yamaguchi K (2013) Research on the prognostic risk of baby cell for Guerilla-heavy rainfall considering by vorticity with Doppler velocity. *J Hydraul Eng JSCE* 57:307–312
5. Tachikawa Y, Nagatani G, Takara K (2004) Development of stage-discharge relationship equation incorporating saturated–unsaturated flow mechanism. *Ann J Hydraul Eng JSCE* 48:7–12 (in Japanese with English abstract)

6. Tachikawa Y, Esaki S, Shiiba M, Ichikawa Y (2009) Rainfall-runoff analysis of the Toga river flush flood in July 2008 to prevent the water accident. *J River Eng JSCE* 15:43–48
7. Yu W, Nakakita E, Kim S, Yamaguchi K (2015) Improvement of rainfall and flood forecasts by blending ensemble NWP rainfall with radar prediction considering orographic rainfall. *J Hydrol.* doi:[10.1016/j.jhydrol.2015.04.05](https://doi.org/10.1016/j.jhydrol.2015.04.05)